Charentaise distillation of cognac. Part II: Process simulation and impact of recycling practices on the aroma composition of freshly distilled spirit

Gabriela Zanghelini, Violaine Athès, Stéphane Vitu, Pierre Giampaoli, Martine Esteban-Decloux

Charentaise distillation of cognac. Part II: process simulation and impact of recycling practices on the aroma composition of freshly distilled spirit

Gabriela Zanghelini[a*], Violaine Athès[a], Stéphane Vitu[a,b], Pierre Giampaoli[a] and Martine Esteban-Decloux[a]

[a]Université Paris-Saclay, INRAE, AgroParisTech, UMR SayFood, 91120 Palaiseau, France
[b]CNAM, 75003 Paris, France
*Corresponding author

Email adresses: gabriela.zanghelini@agroparistech.fr (G. Zanghelini), violaine.athes-dutour@inrae.fr (V. Athès), stephane.vitu@lecnam.net (S. Vitu), pierre.giampaoli@agroparistech.fr (P. Giampaoli), martine.esteban-decloux@agroparistech.fr (M. Esteban-Decloux).

Publié dans Food Research International (178) 113861
https://doi.org/10.1016/j.foodres.2024.113861

ABSTRACT

A growing number of studies over the years has successfully employed computer simulation tools to understand, optimize and design spirit distillations. Amongst distilled spirits, cognac is a reputed wine spirit resulting from a double batch distillation process known as Charentaise distillation. This complex operation comprises the wine distillation (WD) and the brouillis distillation (BD), which are carried out in copper alembics. The distillate produced in each batch is fractionated and some of those fractions are recycled in subsequent batches. To improve the current understanding of the behavior of aroma compounds during the process, computer simulation modules were built in this work for a WD and a BD and the results were compared with experimental data. Of the 62 aroma compounds detected in the samples over time, 52 could be represented in the simulations, including 37 using the NRTL thermodynamic model to calculate vapor-liquid equilibria and another 15 with the UNIFAC model. Half of those had their concentration profiles and their partitioning accurately described by the simulation, most of which were modeled with NRTL. This highlights the need for reliable vapor-liquid equilibrium data for aroma compounds that were poorly represented or absent from the simulation as well as kinetic data for chemical reactions occurring during distillation. Furthermore, the impact of the recycling operation on the composition in aroma compounds of freshly distilled cognac was investigated. To represent a steady state, a mathematical model was employed to implement the recycling of distillate fractions during 8 successive Charentaise distillation cycles. The operation was shown to improve the extraction of ethanol and of all volatile compounds in the heart, reaching a pseudo steady state after 3 to 5 cycles. The recycling of the second fraction had a higher influence on the extraction of alcohols and terpenes, while for most esters and norisoprenoids the recycled head fractions played a bigger role.

Keywords: cognac; batch distillation; aroma compounds; computer simulation; distilled spirits; recycling.

1. INTRODUCTION

Cognac is a reputed wine spirit whose distinctive aroma bouquet is the result of the interplay of hundreds of aroma compounds that are present at different concentrations in an ethanol-water matrix. The beverage is traditionally produced from a double batch distillation operation known as Charentaise distillation, which consists of two consecutive steps: the wine distillation (WD) and the brouillis distillation (BD).

In the WD, the wine is distilled for approximately 11 h into three fractions of distillate that are collected separately: the head, the brouillis and, often, the tail. The brouillis produced in three different WD is collected and distilled for 12 – 14 h in the BD, resulting in four distillate fractions: the head, the heart, the second and the tail. The heart corresponds to the freshly distilled spirit or unaged cognac, which contains up to 73.7% v/v ethanol and most of the compounds responsible for cognac aroma before being stored in oak barrels for aging. The heads contain the most volatile compounds such as acetaldehyde and ethyl acetate, which are characterized by strong pungent smells, as well as fatty acid-copper complexes that formed in the previous batch and were solubilized by the high ethanol content of the first liters of distillate, conferring a blueish coloration to the heads (Guymon, 1974; Tsakiris et al., 2016). The tails, on the other hand, gather the less volatile compounds such as long-chain fatty acids, which are characterized by soapy and fatty aromas (Guymon, 1974). The aqueous mixture remaining in the boiler after each distillation is the residue.

The goal of the distillation operation is to favor the presence of positive aromas in the heart fraction while limiting the presence of compounds that are considered as off-flavors. In practice, this can prove to be quite a complex task as several different factors intersect to define compound separation during distillation. These might include intrinsic chemical properties of the different constituents of the mixture (Léauté, 1990), the composition of the matrix (i.e., the ethanol concentration) and operation conditions such as the heating power. In essence, distillation remains an equilibrium-based separation process that is driven by heat-induced deviations from a state of thermodynamic equilibrium between the liquid and the vapor phase above it towards a new state of vapor-liquid equilibrium (Valderrama et al., 2012).

To improve the extraction of ethanol and of aroma compounds in the heart fraction, the heads, tails and second that are separated in the process are recycled into a subsequent distillation. Typically, the heads and tails collected from the WD and the BD are mixed with the wines of subsequent WD and the second is recycled into the brouillis of a following BD. Alternatively, some distilleries prefer to recycle the second fraction in a subsequent WD instead of a BD. Recycling practices avoid the loss of ethanol and of flavor compounds that would otherwise be wasted.

Despite the long history of this recycling operation in spirit distillation, it is seldom considered in the literature and only a few studies to date have investigated its impact in the

aroma composition of the heart. In a study concerning a batch column distillation of a brouillis for the production of grappa, da Porto et al. (2010) observed that the recycling of heads and tails enriched the freshly distilled grappa in ethanol, esters, aldehydes and alcohols. However, since the effect was only assessed for a single recycling and a limited number of compounds, the results should be interpreted with caution. More recently, Esteban-Decloux et al. (2021) examined the effects of recycling for pilot-scale double batch distillations of cider for the production of Calvados. When comparing the hearts of the first and the second brouillis distillations, the authors found that only compounds markedly present in the second fraction increased in concentration from one heart to another, whereas the recycling of heads and tails had little effect. However, no scenarios in the total absence of recycling were tested for comparative purposes. Here again, due to the high material costs, recycling was only performed for 9 cider distillations and 2 BD. This means that a steady state was likely not achieved for the BD, making it hard to draw any conclusions on the impact of a consistent recycling operation.

A less dispendious and less time-consuming alternative to study the impact of spirit distillation parameters on the behavior of volatile aroma compounds is the use of computer simulation. Designing and simulating distillation processes requires the knowledge of vapor-liquid equilibrium (VLE) data for the multiple components in the system coupled to an adequate thermodynamic model to perform the mass and energy balances, in addition to structural and temperature-dependent properties of the different components (Valderrama et al., 2012). In the case of spirit distillation, the system consists of multicomponent mixtures of aroma compounds highly diluted in an ethanol-water matrix.

An increasing number of studies over the last decades have successfully employed simulation tools to understand, optimize and design continuous and batch spirit distillations. Some of these studies focused on investigating the influence of different distillation parameters on the behavior of volatile compounds (Batista & Meirelles, 2011; Esteban-Decloux et al., 2014, 2022; Hodel et al., 2021; Puentes et al., 2018b; Sacher et al., 2013; Scanavini et al., 2012), while others sought to increase the yield of ethanol and compounds with positive aroma notes and to minimize the extraction of deleterious and undesired compounds (Luna et al., 2018, 2019; Osorio et al., 2005). Regarding cognac production, Douady et al. (2019) simulated the behavior of 26 volatile compounds during batch distillations of a brouillis in a pilot-scale (600 L) copper alembic and of a wine without lees and a brouillis in an industrial-scale (25 hL) copper alembic; however, the study focused in each case on a single distillation, for which no recycling was performed.

With that in mind, the present study is the second of a two-part study concerning the behavior of aroma compounds during a Charentaise distillation for the production of cognac. While part 1 (Zanghelini et al., 2024) focused on experimental results, this second part introduces the performance and flexibility of computer simulation tools to help elucidate the impact of different distillation parameters and particularly of the recycling operation on the

behavior of volatile aroma compounds during a Charentaise distillation for the production of cognac. The first step was to build simulation modules for the WD and the BD of an experimental Charentaise distillation and compare the results with previously published experimental data. Then, a mathematical approach was employed to investigate how the recycling of distillate fractions over 8 successive Charentaise distillations (i.e., 24 WD and 8 BD) affects the chemical composition of freshly distilled cognac.

2. EXPERIMENTAL SECTION

The experimental distillation process consisted of two consecutive batch distillations in an industrial-scale copper Charentais alembic with a filling capacity of 25 hL (2.5 m^3): the wine distillation (WD) and the brouillis distillation (BD), as described in Zanghelini et al. (2024). Both distillations included recycling of distillate fractions from previous distillations using the same wine batch. Distillate flow rate, density, alcoholic strength and temperature were recorded every 10 s by a Coriolis flowmeter (Proline Promass E 300, Endress+Hauser) attached to the hydrometric port of the alembic. Gas pressure and temperatures in different parts were also recorded every 10 s. These recorded data were essential for the design of the simulation modules built in this study.

2.1. Analyses of volatile compounds

The different samples analyzed in the study included distillate samples collected over time for both the WD and the BD, in addition to the boiler loads (wine + recycled heads and tails or brouillis + recycled seconds) and the residues.

2.1.1. Alcohol strength

The alcohol strength of the samples was determined from density measurements at 20 °C using an oscillating tube density meter (Snap 50, Anton Paar). The conversion from density to ABV (alcohol by volume) was based on the Alcoholometric Tables from the International Organization of Legal Metrology (*International Alcoholometric Tables, OIML R22*, 1975) and considered the samples as ethanol-water mixtures whose density is not influenced by the highly diluted aroma compounds.

2.1.2. Sample preparation

Before the chromatographic analyses, all distillate samples were adjusted to an ABV of 40% v/v to prevent matrix effects, which could induce measurement variations. For the wine samples, the residues and the load of the WD, a preparatory step consisting of laboratory-scale low pressure distillations adapted from Awad et al., (2017) and described in the first part of the study (Zanghelini et al., 2024) was performed prior to analyses. The procedure allows to clear the samples of residual dry matter and increase the concentrations of ethanol and aroma compounds for analysis while preventing the occurrence of thermally induced chemical reactions by maintaining low temperatures during the low pressure distillations.

2.1.3. Analysis of aroma compounds by GC-FID

The volatile compounds, namely alcohols, esters, aldehydes, terpenes and norisoprenoids, were analyzed by a gas chromatograph (GC) equipped with a flame ionization detector (FID) and an automatic sampler as described by Zanghelini et al. (2024). The analysis parameters are provided in the appendix. The chromatographic data were acquired and analyzed using ChemStation software version B.04.03(16) (Agilent). Limits of quantitation (LOQ) were computed using the signal-to-noise method.

2.2. Creation of computer simulation modules for Charentaise distillation

The operation consisted of two consecutive batch distillations (the WD and the BD) as described in Zanghelini et al. (2024). A computer simulation module was created for each of the two steps of the experimental Charentaise distillation using the software BatchColumn (ProSim, France). The vapor-liquid equilibria (VLE) of the multicomponent system was modeled using a heterogeneous thermodynamic approach (γ—φ), in which the gas phase was represented by the ideal gas law and the non-ideality of the liquid phase was computed by the activity-coefficient model NRTL (Non-Random Two-Liquid), as recommended in the literature for similar systems (Valderrama et al., 2012). The NRTL interaction parameters for the binary systems ethanol-water, ethanol-aroma compound and water-aroma compound were obtained from the literature (Puentes et al., 2018a) and from the authors' recent works (Zanghelini et al., 2022a; Zanghelini et al., 2022b) and are listed in the supplementary information. In addition to ethanol and water, 29 aroma compounds were described by the NRTL model. Among the aroma compounds lacking NRTL parameters, 15 were represented by a predictive group contribution model (Modified UNIFAC Dortmund 1993 (Gmehling et al., 1993)). Some of the aroma compounds analyzed in the experimental distillations were not considered in the simulation modules due to a lack of NRTL parameters and the non-availability of the elemental UNIFAC groups required for their decomposition.

The simulation parameters were based on the data recorded by the Coriolis flowmeter during the experimentations and included the recorded variations in the gas pressure. In the simulation modules, the alembic was represented by a batch column consisting of 7 trays, in which tray 1 is the coil condenser, tray 7 is the boiler and intermediary trays 2-6 are theoretical trays that account for the variations in heat loss throughout the different parts of the Charentais alembic with varying diameter and shape. Although no reflux was imposed in the modules, the internal reflux resulting from the partial condensation of vapors due to heat losses was taken into consideration by defining small values of liquid holdup in the intermediary trays and by adjusting tray efficiency accordingly. The different distillation parameters are listed in **Table 1**. The distillation was divided into multiple stages in the simulation modules to account for variations in the distillation parameters during the process. These different stages are illustrated in the supplementary information

2.3. Modeling successive Charentaise distillations with recycling

The Charentaise distillation for the production of cognac typically involves redistilling the head, tail and second fractions in subsequent distillations as a means to recover the ethanol and compounds of interest that would otherwise be lost. To assess the actual impact of this recycling operation over consecutive distillations on the chemical composition of the heart fraction, 24 WD and 8 BD were modeled using a series of mathematical calculations, which are listed in the supplementary information. The model is based on the repartition of components between the different distillate fractions during the WD and the BD and the initial composition of the wine loaded into the boiler. This approach considers the double batch distillation as a system in which wine is loaded to produce the heart after three consecutive wine distillations and one brouillis distillation, as detailed below.

The total load volume for all the WD was estimated considering that the total load volume in the BD must never exceed 25 hL (2.5 m^3), which is the maximal boiler capacity allowed by the AOC regulations for cognac (Ministère de l'agriculture et de la souveraineté alimentaire, 2022). The distillations were modeled as illustrated in **Figure 1**. In the first distillation, WD_1, the load was composed solely of wine, producing head (H_{WD1}), brouillis (B_{WD1}), tail (T_{WD1}) and residue (R_{WD1}). For WD_2, the load consisted of the wine, H_{WD1} and T_{WD1}, to produce H_{WD2}, B_{WD2}, T_{WD2} and R_{WD2}. Likewise, in WD_3 the wine, H_{WD2} and T_{WD2} were distilled into H_{WD3}, B_{WD3}, T_{WD3} and R_{WD3}. The brouillis from the three WD (B_{WD1}, B_{WD2} and B_{WD3}) were loaded in the boiler for BD_1, which resulted in head (H_{BD1}), heart (Ht_{BD1}), second (S_{BD1}), tail (T_{BD1}) and residue (R_{BD1}). For WD_4 to WD_6, in addition to the wine and the head and tail from the previous WD, the load included ⅓ of H_{BD1} and T_{BD1}. Similarly, the load of BD_2 consisted of B_{WD4}, B_{WD5}, B_{WD6} and S_{BD1}. The subsequent distillations were modeled following the same logic.

The following assumptions were considered in the model:

- All the distillate fractions are entirely recycled after 3 WD and 1 BD.
- The total load volume in the WD and BD must not exceed 25 hL; accordingly, the volumes of wine loaded for the WD are increasingly smaller as the volume of the recycled fractions increases with each distillation.
- The only matter leaving the system are the heart and the residues from the WD and the BD.
- The distribution of volatile compounds between distillate fractions is constant for each type of distillation (WD and BD), as their partitioning is a function of their volatilities at different ethanol concentrations in the boiling liquid.

3. RESULTS AND DISCUSSION

The results discussed in this section are presented in two subsections, which comprise: (1) the simulation of the two steps of a Charentaise distillation and comparison with experimental data; (2) the impact of the recycling operation on the composition of the heart fraction in relation to that of the base wine.

3.1. Simulation of a Charentaise distillation

The mass concentration profiles obtained from the simulations of the WD and the BD for ethanol and for a few representatives of aroma compounds are contrasted with experimental data in **Figure 2** (alcohols and esters) and **Figure 3** (aldehydes, terpenes and norisoprenoids), in which the distillate cuts are denoted by vertical dashed lines. The simulations were performed considering two case-scenarios: one using the initial concentrations determined experimentally in the boiler loads (WD = wine + recycled heads and tails; BD = brouillis + recycled second), x_0, and another in which the final mass of each compound is used to estimate its initial concentration in the load, x_f, so as to account for the compound formation observed experimentally during the WD and/or the BD (Zanghelini et al., 2024). The initial concentrations for both approaches in the WD and in the BD are listed in **Table 2**. For compounds that were present in the distillate but were below their limits of quantitation (LOQ) in the boiler load, their initial concentration was set to 1.00E-8 $g \cdot g^{-1}$.

Alcohols

The concentration profiles of alcohols and their repartitions between the distillate fractions were overall well-represented by the simulations using NRTL, as observed in Figure 2(c-d). A good correspondence was obtained between the simulations and the experimental data in the WD, whereas in the BD the concentrations in the head and in the heart are slightly underestimated for the three alcohols depicted, especially for methanol. A relatively good correspondence was also observed for 2-methylbutan-1-ol, 3-methylbutan-1-ol, (*Z*)-3-henexol and 2-phenylethanol (data not shown), although the concentration of the latter was overestimated in the WD. Amongst alcohols, only butan-1-ol and hexanol were not well represented by the simulation. Butan-1-ol was below its LOQ in the charges in most of the samples and the initial concentration of 1.00E-8 $g \cdot g^{-1}$ considered in the simulations might have been incompatible with the experimental distillations. As for hexanol, although its simulation profile was somewhat similar in shape to the experimental one, its maximum concentration was underestimated in the heads and in the heart and overestimated in the second and tails. This is likely due to inconsistent VLE data, given that poor representations for this compound was also observed in the works of Douady et al. (2019) using the same NRTL coefficients.

UNIFAC predictions gave a fairly close representation of the overall trend and distributions for octanol, decanol and dodecanol for both the WD and the BD, but underestimated the concentrations of tetradecanol and hexadecanol in the WD (data not shown). This could be related to the structural differences between the C_8-C_{12} alcohols and the more complex long-chain alcohols. The UNIFAC model is a group contribution method which considers that a mixture is characterized by the added contributions of its molecules' functional groups. As a corollary, it assumes that all functional groups are independent from one another (Muzenda, 2013). While this simplifying assumption can be reasonable for simpler mixtures involving molecules such as short- to mid-chain alcohols, it often fails to accurately represent more

complex systems containing molecules such as longer-chain alcohols, in which interactions between groups are likely more significant.

Esters

Amongst esters, the concentration profiles of ethyl acetate and ethyl lactate, obtained by simulation were rather close to the experimental profiles. This was also the case for ethyl butyrate, isoamyl acetate and ethyl 3-methylbutanoate (ethyl isovalerate), although the concentration in the head was underestimated for the last two in the WD when the initial concentration x_0 is considered (data not shown). The profiles of ethyl octanoate (Figure 2(e-f)), and ethyl decanoate (data not shown) presented a similar shape, but with overestimated concentrations for the entire BD. This could be linked to a degradation of these compounds during distillation, either from temperature-catalyzed hydrolyses or from the saponification of the compounds with copper ions from the alembic walls (Schaefer & Timmer, 1970; Zanghelini et al., 2024). This potential degradation cannot be accounted for in the simulation unless the corresponding chemical reaction is added to the module, leading to a higher recovery of the compounds predicted by the simulation than that observed experimentally.

Esters whose experimental concentration profiles were not well represented in the simulations of both distillations were diethyl succinate, ethyl hexanoate and hexyl acetate, as well as esters modeled with UNIFAC (data not shown). Differently from alcohols, the predictive model UNIFAC performed poorly for all the esters, likely due to the more complex structure of esters (Muzenda, 2013). In the case of esters represented by the NRTL model, the disparities could be due to a degradation not accounted for in the simulation (as noted in the experimental results for ethyl hexanoate and hexyl acetate (Zanghelini et al., 2024)) or to inconsistencies in the VLE data available in the literature for these compounds.

Aldehydes, Terpenes and Norisoprenoids

While aldehydes (Figure 3 (a-d)) were well represented by the simulations for the BD, their simulated and experimental concentrations were markedly different during most of the WD. This is likely a consequence of the substantial formation of these compounds observed throughout distillation, which is not taken into account in the simulation module.

The disparities between experimental and simulated data were particularly marked for furfural (Figure **3**(c-d)), which showed a linear increase in the experimental concentration during the WD while the simulated data suggest the opposite trend, with a linear decrease from the same initial concentration until the compound is nearly exhausted from the boiler. This is in accordance with the findings of Ikari & Kubo (1975), who observed a similar growing concentration profile for furfural during the experimental distillation of a whisky mash, while this increase was not present in the researchers' simulations of their distillation. Contrastingly, during the BD, in which no furfural formation occurred, the experimental and simulated concentration curves for furfural are practically overlapped; this confirms that the NRTL parameters can provide a good representation of the compound in the system in the absence of chemical reactions. This ineptness of the simulation modules to properly represent compounds formed or degraded during the distillation also applied for

(*E*)-ß-damascenone, α-terpineol and linalool, whose concentrations were highly underestimated by the computer simulation during the WD but were well represented in the BD (Figure **3**(e-f)).

While in theory chemical reactions could be added to simulation modules in the form of stoichio-kinetic models, this would require not only determining which precursors are responsible for the formation of each compound, but also knowing the specific reaction kinetics in distillation conditions. Such data are not readily available in the literature and experimental determinations of reaction kinetics can be rather dispendious and time-consuming. Moreover, some volatile compounds have more than one formation pathway which can involve multiple potential precursors, many of which are non-volatile and quite challenging to quantify in the wine. With this in mind, we tested if using x_f as the initial concentrations for newly-formed and degraded compounds in the computer simulations could provide a quick alternative to improve their representation when adding chemical reaction kinetic models to the simulations is not possible.

A comparison between the simulation using the initial concentration (x_0) and that using the concentration based on the final mass (x_f) is illustrated for furfural, α-terpineol, (*E*)-ß-damascenone and linalool in Figure **3**. The approach using x_f considers that, for a given compound, all the additional mass derived from chemical reactions is present in the boiler from the beginning of distillation. In the same logic, in the case of degraded compounds, it considers that the mass lost due to degradation was absent from the beginning. Consequently, it works fairly well for compounds that form or degrade early on, but less well for compounds that are formed or degraded mostly in later stages of the distillation. For instance, (*E*)-ß-damascenone and α-terpineol are likely products of acid-catalyzed hydrolyses of glucosides in the WD (Dziadas & Jeleń, 2016; Waterhouse et al., 2016), and thus could form rapidly from the beginning of distillation. Consequently, the approach using x_f allows to slightly improve their representation by the simulation module, as seen in Figure **3**(g). A slight improvement was also noted in the BD (Figure 3(h)), during which the slight increase observed in their masses seems to be compensated in the simulation by using x_f for the boiler load, even if the two compounds were not considered as formed in the BD (Zanghelini et al., 2024). On the other hand, furfural and isobutanal are known to be formed from thermal degradations that are expectedly more intense with the increasing distillation temperature over time; as such, the formation of these compounds is minimal in the initial stages of distillation and grows increasingly important throughout the distillation. As a result, the simulation of the WD using the final masses highly overestimates their initial concentrations and, consequently, underestimates their concentrations in the later stages of distillation.

The capability of the simulation to represent the experimental behavior of aroma compounds was judged based on two factors: (1) the shape and amplitude of the concentration profiles and (2) the repartitions of compounds between distillate fractions.

The resemblance between the simulated and experimental concentration profiles is evaluated in **Table 3** as great (+++), good (++), close (+), overestimated (>), underestimated (<) or wrong shape (Ø).

The compounds whose simulation results best resembled the experimental data were alcohols and short-chain esters, especially those represented by the NRTL model. The simulation of the BD gave overall better results than the WD. This likely reflects the enhanced presence of chemical reactions in the WD than in the BD, as observed by Zanghelini et al., (2024) and Awad et al. (2017). Using x_f for the initial concentration in the simulation modules allowed to improve the resemblance between the experimental and simulated concentration profiles of newly-formed compounds such as terpenes and norisoprenoids, as well as esters that were substantially degraded (with final masses corresponding to 66% of their initial masses or less), such as ethyl octanoate and ethyl decanoate, and compounds not quantified in the charge of the WD, such as butan-1-ol. However, it offered little improvement for the fitting quality for formed esters and aldehydes.

A comparison between the experimental and simulated repartitions for the compounds used in the simulation module is detailed in **Table 4**. Given that the repartitions between the distillate fractions were practically the same regardless of the concentrations used in the boiler load of the simulation, only the repartitions using x_0 are presented in the table. Compounds whose repartitions were best represented by the simulation were short-chain alcohols (except hexanol), ethyl lactate and 2-phenylethyl acetate. Octanol, dodecanol, (*E*)-ß-damascenone, linalool, and α-terpineol were also quite well represented in the WD and their experimental and simulated repartitions showed minor discrepancies during the BD. Similarly, 2-phenylethanol, decanol and tetradecanol were still relatively well represented by the simulation, with minor discrepancies for both distillations. Finally, compounds whose simulated repartitions resemble less well the experimental data in both distillations include hexadecanol, isobutyl acetate, diethyl succinate, ethyl decanoate, ethyl dodecanoate, ethyl linoleate, ethyl oleate, ethyl octadecanoate and most aldehydes, most of which were described using UNIFAC due to a lack of experimental VLE data.

3.2. How recycling distillate fractions impacts the composition of the freshly distilled spirit

The recycling of distillate fractions into the distillation load is seldom considered in studies concerning spirit distillation. One of the reasons behind this is the high number of experimental distillations and thus high material costs and laboriousness that such a study would involve. With this in mind, this study proposed to employ a faster, more flexible and more cost-effective approach to estimate the effect of recycling based solely on the experimentally determined initial composition of the wine and on the repartitions between distillate fractions.

For compounds whose masses increased or decreased considerably during distillation (as listed by Zanghelini et al. (2024)), their initial concentration was estimated based on the final masses (x_f), as described in the previous subsection. Whenever possible, the repartition of components obtained by computer simulation for each compound was favored over the experimentally determined ones to avoid any inconsistencies in the mass balances that might arise from analytical issues. However, in cases in which computer simulation was not applicable (e.g., due to a lack of VLE data in hydroalcoholic mixtures) or failed to accurately represent the behavior of compounds (e.g., for compounds formed during distillation), the experimental repartitions from Zanghelini et al. (2024) were used instead. Some of the compounds that were quantified in the experimental distillations but that were missing in the simulation modules due to a lack of VLE data and the non-applicability of the UNIFAC model were also included, in which case the experimental repartitions were used as well. To ensure that a steady state would be reached, 8 consecutive Charentaise distillations were assessed, including 24 WD and 8 BD.

The model considered that the head and tail fractions from each WD were recycled in a subsequent WD, that ⅓ of the head and tail from each BD were mixed with each of the wines of three subsequent WD and that all seconds were redistilled with the brouillis in a subsequent BD, as illustrated in Figure 1. The WD load in the model was kept at a constant volume that was estimated so that, once a steady state was reached, the volume of the BD load was lower or equal to 25 hL.

The impact of this recycling configuration on the extraction of ethanol and aroma compounds into the hearts was examined by comparing the recovery percentages after 8 successive BD employing the traditional recycling of heads (H) and tails (T) in the WD and of the second (S) in the BD (R-HST) with a configuration with no recycling (NR), as listed in **Table 5**. The partitions of compounds between distillate fractions used for this comparison depended on their simulation quality, as described above. The repartition used for each compound (experimental or simulated) is listed in the first column of Table 5.

Initially, the case of a recycling of all distillate fractions was considered (R-HST), since it is the most common scenario. When compared to the composition of the wine, the heart fraction at the end of 8 successive BD contains 98.8% of the initial mass of ethanol, 92.4% of the methanol and more than 99.7% of most alcohols, with the exception of 2-phenylethanol (9.0%), farnesol (65.4%) and hexadecanol (88.3%). It also contains 79-100% of most esters, except for ethyl lactate (42.9%) and diethyl succinate (57.4%), and at least 95.6% of terpenes and norisoprenoids, aside from (*E*)-nerolidol with 70.2% extraction.

If no distillate fractions were recycled (NR) in the double batch distillation, the recovery of all compounds would be substantially smaller and only 72.1% of the ethanol initially contained in the wine would be recovered in the heart, resulting in a substantial financial impact due to the loss of ethanol. The lack of recycling could also significantly impact freshly

distilled cognac aroma, since the extraction of all aroma compounds in the heart would be lower, with ≤88.0% of alcohols, ≤83.4 % of esters and ≤88.1 % of terpenes and norisoprenoids. On the other hand, omitting the recycling would limit the presence of undesirable compounds in the heart. This is the case for methanol, a potentially toxic compound whose extraction would decrease from 92.4% to merely 55.2%, and TDN, a kerosene-scented compound whose extraction would be limited to 58.5% instead of 95.6%. These increased extraction percentages with the multiple recycling have also been observed in other studies in the literature for experimental distillations of grappa (da Porto et al., 2010) and cider (Esteban-Decloux et al., 2021).

To better understand how the recycling of different fractions increases the extraction rate, different recycling configurations were tested and compared with the traditional recycling (R-HST) (Table 5). One case scenario is the recycling of the second fraction in the WD (R-HST$_{WD}$), a configuration that is adopted by some distilleries instead of the more traditional R-HST. When comparing the two configurations, the R-HST$_{WD}$ revealed to give similar results to the traditional R-HST for the majority of compounds and only differed for compounds which are partially evacuated in the residue (e.g., methanol, 2-phenylethanol, furfural, ethyl lactate and diethyl succinate), who presented lower recovery rates in the R-HST$_{WD}$ configuration. Because such compounds are mostly present in the second, tails and residues, recycling the second in the WD increases their mass in the load of the WD; as a result, increasing amounts of these compounds are evacuated in the residue with each distillation cycle, lowering their extraction in the heart while increasing the energy consumption. This would likely also be the case for carboxylic acids, which are extracted at the final hours of distillation (Douady et al., 2019; Zhao et al., 2014).

The recycling of the second fraction played the biggest role in increasing the extraction of most alcohols (except 2-phenylethanol and long-chain alcohols), as well as α-terpineol, (*E*)-ß-damascenone, ethyl furoate, 2-phenylethyl acetate and 2-phenylethyl octanoate. This was the case both when the second is recycled in the WD (R-HST$_{WD}$) and in the BD (R-HST).

Another case scenario tested involved the recycling of only second and tails (R-ST), and thus no recycling of the heads. Separating the heads from the rest of the distillate is essential to "rinse" the coil pipe of the alembic from any residual fatty acids that might have remained from the previous distillation and would risk ending up in the brouillis and heart, as explained in Zanghelini et al. (2024). However, given that the head fraction is highly concentrated in compounds that are associated with strong and often unwanted aroma notes, its recycling in the WD might negatively impact the aroma of the heart. A comparison between the traditional recycling and R-ST shows that the recycling of the heads plays in fact an important role in the recovery of esters and most norisoprenoids, also contributing to the extraction of alcohols and, particularly, of ethanol, which increases from 94.8% to 98.8% when heads are recycled. This is quite surprising, considering that heads only represented 4% of the total mass of the head + tail mixture recycled in the WD, but can be explained by

the substantially higher amounts of most esters in the heads (as exemplified by Figure 2(e-f)). Given that most esters and norisoprenoids are associated with floral and fruity notes, it can be inferred that the recycling of the head fraction has an overall positive impact in the composition of the heart and that discarding the heads instead of recycling them would likely have negative consequences to the aroma of the freshly distilled cognac. On the other hand, this recycling also improves the extraction of compounds such as ethyl acetate, which is associated with a strong nail polish aroma and, if present in high amounts, might negatively impact cognac aroma (Guichard et al., 2003; Spaho et al., 2019).

On this regard, it is interesting to highlight that the recycling of heads only slightly impacted the extraction for methanol - an ill-reputed and potentially toxic compound that is often argued to be concentrated in the head fraction. Although many sources in the literature over the last decades suggest that separating the heads limits the amount of methanol in the heart fraction (Scanavini et al., 2012; Silva & Malcata, 1999), these results show not only that methanol is present in all distillate fractions (Figure 2(b-d)), as demonstrated in other works in the literature (Balcerek et al., 2017; Botelho et al., 2020; Carvallo et al., 2011), but also that discarding the heads would have little impact on its presence in the heart.

Finally, a configuration with recycling of the second fraction exclusively (R-S) was considered, i.e., no recycling of heads nor tails. This configuration resulted in extraction rates that were quite similar to the R-ST configuration in most cases. However, for compounds with an increased presence in the tails fraction (e.g., 2-phenylethanol, ethyl lactate, diethyl succinate and methyl salicylate) the R-S recycling led to expressively lower extraction rates, which in some cases were nearly as low as in the NR case scenario.

In sum, these results show that, regardless of the recycling configuration, the recycling of distillate fractions improves the extraction of all aroma compounds in the heart, including those partially evacuated in the residues. As denoted in Table 5, the contribution of the different distillate fractions to this increase is quite variable depending on the partitioning of each aroma compound during distillation. In general, the recycling of the second fraction was more influential in the extraction of alcohols and terpenes, while for most esters and norisoprenoids the recycled heads played a bigger role. Furthermore, compounds with high recovery percentages in the hearts after 8 BD were those which partitioned mostly into the brouillis in the WD and in the heart and second in the BD. Contrastingly, compounds with low extractions in the heart such as 2-phenylethanol and benzaldehyde are those that distill mostly in the final hours of distillation and are partially lost in the residue.

On the other hand, this increase in the extraction of aroma compounds from the wine into the hearts does not always translate into an increase in concentration. The recycling of all heads and tails into the wine resulted in progressively smaller volumes of wine being loaded in the boiler to comply with the constant total load volume stipulated for the WD. This constant volume was estimated so that, once a steady state was reached, the volume of the

BD load never exceeded 25 hL (Ministère de l'agriculture et de la souveraineté alimentaire, 2022). This step was important since the volume load of the BD increased with each recycling, given that it consisted of all the brouillis produced in three consecutive WD plus the second from the previous BD. Thus, with each recycling of the second fraction, a relatively steady volume of brouillis was loaded into the alembic, producing a higher second volume in each cycle and, hence, resulting in an increasingly higher load volume in the subsequent BD. This higher load volume led to a decrease in concentration in the hearts of the 8 BD for several of the aroma compounds, even if their extraction rates increased from the Ht_{BD1} to Ht_{BD8}. This is illustrated in **Figure 4**, which shows the concentrations of different aroma compounds in the hearts of the 8 BD considered in the model, in addition to the evolution of the volume load for the 8 BD.

To evaluate the capability of the approach proposed in this study to represent industrial distillations with recycling, the concentrations, in grams per gram of ethanol ($g \cdot g_{Et}^{-1}$), of the different compounds considered in the model (filled symbols) were compared with their experimental concentrations (hollow symbols) in the hearts sampled over four days from a cognac distillery (Figure 4(b-g)).

As observed in Figure 4(a), the recycling of distillate fractions increased the total loaded volume in each BD in the first distillation cycles and a plateau was reached after 3 cycles. Regarding aroma compounds, the main factor determining if their concentrations increase or decrease in the heart after 8 BD is their distribution between distillate fractions. Compounds which tended to increase in concentration in the hearts with recycling were those which partitioned into the second fraction, especially if they were also significantly present in the tails. This is not surprising, considering that the recycled second corresponds to 18% of the initial mass of the BD and 21% of the ethanol, whereas only 14% of the initial mass and 10% of the ethanol from the WD are represented by the recycled heads and tails. The compounds with the highest increases in concentration over 8 BD are diethyl succinate, 2-phenylethanol, ethyl lactate, isobutanal, furfural and 1,1-diethoxyisobutane, whereas compounds such as methanol, ethyl formate, ethyl furoate, 2-phenylethyl acetate, α-terpineol, (*Z*)-linalool oxide and (*E*)-linalool oxide presented only slight increases in concentration. Similar results were observed by Esteban-Decloux et al. (2021) for the production of Calvados. The authors found that most aroma compounds decreased in concentration after two consecutive brouillis distillations with recycling and only compounds with a significant presence in the second fraction presented a higher concentration in the heart.

The concentrations of aroma compounds in relation to ethanol in the heart of the eight BD reached a pseudo steady state after 3 to 5 successive BD. This corroborates the results of Chiotti et al. (1993), who proved that multicomponent batch column distillations with the recycling of intermediary distillate fractions converge to a "steady state" balance after only 4 or 5 distillation operations. In their study, the authors were among the first to demonstrate

that multicomponent batch distillations can be modeled in a simplified approach such as the one proposed here without the need for consecutive simulations to reach the steady state.
In terms of cognac aroma, recycling over several distillation cycles can be deemed to have a mostly positive impact, since it increases the concentration of furfural, which is associated with smoky and nutty aroma notes, 2-phenylethanol, a rose-scented compound which is a key contributor to the floral aroma of cognac, diethyl succinate, a sweet-smelling ester, and ethyl lactate, which acts as a stabilizer of distillate aromas (Apostolopoulou et al., 2005; Lurton et al., 2012; Tsakiris et al., 2016; Uselmann & Schieberle, 2015; Yuan et al., 2023). It also decreases the concentration of waxy compounds such as decanol, dodecanol, tetradecanol and ethyl tetradecanoate. The potentially negative contribution of recycling to the aroma is milder, driven by slight increases in the concentration of ethyl formate, characterized by green odor notes, and isobutanal, an aldehyde known to impart green and herbal notes (Tsakiris et al., 2014), as well as the decrease in the concentration of citrus- and flower-scented linalool (Thibaud et al., 2020). However, given the small extent of the changes in concentration predicted by the model in most cases, it is worth investigating if this would actually lead to noticeable impacts in the aroma.

In addition to aroma, recycling could have an impact on health, since it increases the concentration of methanol, which can be toxic above certain concentrations (Luna et al., 2018; Tsakiris et al., 2016), and furfural, a potentially toxic compound whose presence is regulated in some distilled beverages (Ramírez-Guízar et al., 2020).

The comparison with experimental data show a good agreement between the model and the experimental data, except in cases such as ethyl formate, ethyl acetate, ethyl lactate, acetaldehyde and TDN. For ethyl acetate and ethyl lactate, for which the simulation data were used in the model, this disparity is likely due to the differences between the experimental and simulated repartitions. For instance, the simulation predicts a smaller loss of ethyl lactate in the residue of the WD and, as a result, higher amounts of the compound are predicted in the hearts by the model than those observed experimentally. For ethyl formate, the lower concentrations predicted by the model are likely due to an additional formation of this compound observed during the experimental BD, which is not taken into account by the model. For acetaldehyde and TDN, both of which are formed in high amounts during the WD, the lower concentrations predicted by the model might also be linked to an inadequacy of the model to compensate for this formation, or even to analytical inconsistencies in the experimental data.

Nevertheless, the recycling model proposed in this work provided a good first approach to gain better insight in the impact of recycling on the composition of freshly distilled cognac. The model could potentially be applied in other studies concerning different distilled spirits for which recycling is employed. For this, a substantial amount of work is still needed to increase the number of aroma compounds whose behavior in hydroalcoholic mixtures can be accurately simulated; this would improve the flexibility and applicability of the model, as

it would require only the distillation data from an online flowmeter attached to the distillation apparatus and the initial composition of the wine.

4. CONCLUSIONS

Computer simulation modules were designed in this work to reproduce a Charentaise distillation for the production of cognac and the results were compared with experimental data. Although a good correspondence was found between the simulated and experimental concentration profiles of ethanol and most alcohols and their distributions between distillate fractions, the simulation failed to accurately predict the behavior of compounds that underwent chemical reactions leading to an increase or decrease in their masses during the process. To improve the performance of the simulation module for these compounds, new concentrations were estimated for the initial alembic load based on the masses of newly-formed compounds at the end of the distillation. While this strategy proved to be rather effective for compounds that were formed from the beginning of distillation (e.g., terpenes and norisoprenoids), it led to larger disparities for compounds that are formed mostly towards the end of the operation (e.g., aldehydes). For the latter, experimental kinetic data need to be measured to improve their representation by the simulation modules.

Due to the limited availability of reliable VLE data for aroma compounds, some of the aroma compounds from the experimental data were not included in the simulation module. In some cases, compounds with no VLE were modeled using the predictive model UNIFAC, which proved to be a reasonable alternative to simulate systems with simple molecules when VLE data are not available, but was not well suited for more complex systems such as those containing long-chain alcohols and esters. Furthermore, UNIFAC lacked the required functional groups to be applicable to molecules such as norisoprenoids. To further increase the number of aroma compounds whose behavior can be correctly described in simulations of distillation operations, more studies are needed to (1) measure reliable VLE data for other aroma compounds and (2) to determine the chemical reactions responsible for the formation of some compounds and measure the kinetic parameters for these reactions to be able to include compound formation in the simulation modules.

A mathematical approach was then used to understand how the recycling of distillate fractions affects the concentrations of aroma compounds in freshly distilled cognac after several distillation cycles. For compounds well represented by the simulation, their initial concentration in the wine and the evolution of ethanol concentration and distillate volume recorded by the flowmeter over time suffice to add them to the model using their simulation partitions. On the other hand, compounds poorly described by or not included in the simulation modules due to a lack of VLE data required experimental repartition data so that they could be accurately represented in the model.

Different configurations for the recycling operation were compared. Overall, recycling allowed to improve the extraction of ethanol and of all volatile compounds in the hearts. The

recycling of all three fractions (heads, tails and second) led to the highest recovery percentages, although each fraction appeared to contribute differently to this increase depending on the partitioning of each compound. For alcohols and most terpenes, this increase was governed by the recycling of the second fraction, whereas for esters and most aldehydes it was the redistilling of heads that played a bigger role. A pseudo steady state was achieved after 3 to 5 brouillis distillations for ethanol and most aroma compounds.

AUTHOR INFORMATION

ORCID
Gabriela Zanghelini: 0000-0001-6993-3878
Violaine Athès: 0000-0002-2194-8517
Stéphane Vitu: 0000-0002-5442-1279
Pierre Giampaoli: 0000-0002-6756-0403
Martine Esteban-Decloux: 0000-0002-8084-2528

Notes
The authors declare no competing financial interest.

Acknowledgements
The authors are thankful to the foundation Jean Poupelain for their financial support and constant assistance. They are also grateful to the Rechou distillery (Angeac-Champagne, France) for their support during the experimental distillations, and the ProSim team for their advisory and technical support with the simulation modules.

Funding
This work was supported by the foundation Jean Poupelain, Javrezac, France.

CRediT authorship contribution statement
G.Z. Methodology, Formal analysis, Investigation, Writing - Original Draft, Writing - Review & Editing, Visualization. **V.A.** Writing - Review & Editing, Supervision, Funding acquisition. **S.V.** Writing - Review & Editing, Supervision. **P.G.** Writing - Review & Editing, Supervision, Funding acquisition. **M.E.D.** Conceptualization, Methodology, Formal analysis, Writing - Review & Editing, Supervision, Funding acquisition.

APPENDIX. GAS CHROMATOGRAPHY METHODS

Analysis of major compounds by GC-FID

The major volatile compounds, namely higher alcohols, esters and aldehydes, were quantified using a gas chromatograph (Agilent 7890A) equipped with a flame ionization detector (FID) and an automatic sampler. The injector and detector were both set to 220 °C. The detector flame was maintained by hydrogen and compressed air at 30 mL·min^{-1} and 320 mL·min^{-1}, respectively. An aliquot of 0.4 µL of sample was injected in split mode (split ratio of 25:1) and carried by a hydrogen flow at 1.4 mL·min^{-1}. The stationary phase was a polar CPWax 57 CB fused silica WCOT column (Agilent, 50 m x 0.25 mm, 0.25 µm). 4-methylpentan-2-ol (CAS 108-11-2) was used as the internal standard at 28 g·L^{-1} in absolute ethanol to minimize system variability between injections. A nitrogen make-up at 25 mL·min^{-1} was employed to improve signal response. The oven was set to 35 °C for the first 5 min, then increased at a linear rate of 4 °C·min^{-1} to 220 °C and held for 10 min.

Liquid-liquid extraction and analysis by GC-FID

A liquid-liquid extraction using isooctane was employed to quantify C_4 to C_{18} ethyl esters, terpenes and norisoprenoids. For the extraction, 1 g of NaCl and 20 mL of adjusted sample were added to a glass flask and placed in the tray of an automated extractor (GX 271, Gilson). A stock solution containing ethyl nonanoate and ethyl tridecanoate at 5 g·L^{-1} in absolute ethanol was added as the internal standard. The extraction was done by adding isooctane to the flasks, agitating for 30 s, then left to decant for 30 min. The organic phase was collected and injected in GC vials for analysis.

The extracts were analyzed in a gas chromatograph (Agilent 6890N) equipped with a flame ionization detector and an automatic sampler. The injector and detector were set to 220 °C. Hydrogen was the carrier gas at 3.3 mL·min^{-1}. Hydrogen and compressed air flow for the FID detector were set to 30 mL·min^{-1} and 400 mL·min^{-1}, respectively. A nitrogen make-up at 28.5 mL·min^{-1} was employed to improve signal response. An aliquot of 1 µL of extract was injected in splitless mode in a DBWax capillary column (Agilent, 60 m x 0.25 mm, 0.25 µm). The oven temperature was initially at 35 °C for 0.7 min, then raised to 60 °C at a linear rate of 20 °C·min^{-1} and held for 3.4 min, and finally increased at 4 °C·min^{-1} to 220 °C and held for 20 min.

Computation of chromatographic data

The chromatographic data were acquired and analyzed using ChemStation software version B.04.03(16) (Agilent). The compounds were identified by comparing their retention times to those of pure standards analyzed under the same conditions. Quantifications were based on calibration curves established from a mixture of reference analytical standards at different concentrations in a hydroalcoholic solution at 40% v/v ethanol. Compounds that were absent from the reference mixture were quantified based on the calibration curves of another compound with similar chemical properties.

REFERENCES

Apostolopoulou, A. A., Flouros, A. I., Demertzis, P. G., & Akrida-Demertzi, K. (2005). Differences in concentration of principal volatile constituents in traditional Greek distillates. *Food Control*, *16*(2), 157–164. https://doi.org/10.1016/j.foodcont.2004.01.005

Awad, P., Athès, V., Decloux, M. E., Ferrari, G., Snakkers, G., Raguenaud, P., & Giampaoli, P. (2017). Evolution of Volatile Compounds during the Distillation of Cognac Spirit. *Journal of Agricultural and Food Chemistry*, *65*(35), 7736–7748. https://doi.org/10.1021/acs.jafc.7b02406

Balcerek, M., Pielech-Przybylska, K., Patelski, P., Dziekońska-Kubczak, U., & Strąk, E. (2017). The effect of distillation conditions and alcohol content in 'heart' fractions on the concentration of aroma volatiles and undesirable compounds in plum brandies. *Journal of the Institute of Brewing*, *123*(3), 452–463. https://doi.org/10.1002/jib.441

Batista, F. R. M., & Meirelles, A. J. A. (2011). Computer simulation applied to studying continuous spirit distillation and product quality control. *Food Control*, *22*(10), 1592–1603. https://doi.org/10.1016/j.foodcont.2011.03.015

Botelho, G., Anjos, O., Estevinho, L. M., & Caldeira, I. (2020). Methanol in grape derived, fruit and honey spirits: A critical review on source, quality control, and legal limits. *Processes*, *8*(12), 1–21. https://doi.org/10.3390/pr8121609

Carvallo, J., Labbe, M., Pérez-Correa, J. R., Zaror, C., & Wisniak, J. (2011). Modelling methanol recovery in wine distillation stills with packing columns. *Food Control*, *22*(8), 1322–1332. https://doi.org/10.1016/j.foodcont.2011.02.007

Chiotti, O. J., Salomone, H. E., & Iribarren, O. A. (1993). Selection of multicomponent batch distillation sequences. *Chemical Engineering Communications*, *119*(1), 1–21. https://doi.org/10.1080/00986449308936104

da Porto, C., Natolino, A., & de Corti, D. (2010). Batch distillation of grappa: Effect of the recycling operation. *International Journal of Food Science and Technology*, *45*(2), 271–277. https://doi.org/10.1111/j.1365-2621.2009.02131.x

Douady, A., Puentes, C., Awad, P., & Esteban-Decloux, M. (2019). Batch distillation of spirits: experimental study and simulation of the behaviour of volatile aroma compounds. *Journal of the Institute of Brewing*, *125*(2), 268–283. https://doi.org/10.1002/jib.560

Dziadas, M., & Jeleń, H. H. (2016). Comparison of enzymatic and acid hydrolysis of bound flavor compounds in model system and grapes. *Food Chemistry*, *190*, 412–418. https://doi.org/10.1016/j.foodchem.2015.05.089

Esteban-Decloux, M., Dechatre, J.-C. C., Legendre, P., & Guichard, H. (2021). Double batch cider distillation: Influence of the recycling of the separated fractions. *Lwt*, *146*(April), 111420. https://doi.org/10.1016/j.lwt.2021.111420

Esteban-Decloux, M., Deterre, S., Kadir, S., Giampaoli, P., Albet, J., Joulia, X., & Baudouin, O. (2014). Two industrial examples of coupling experimentsand simulations for increasing quality and yieldof distilled beverages. *Food and Bioproducts Processing*, *92*(4), 343–354. https://doi.org/10.1016/j.fbp.2013.10.001

Esteban-Decloux, M., Tano, N. G. R., & Grangeon, H. (2022). Study by simulation of the behaviors of volatile aroma compounds during batch multi-stage distillation of spirits. *Journal of the Institute of Brewing*, *Submitted*.

Gmehling, J., Li, J., & Schiller, M. (1993). A Modified UNIFAC Model. 2. Present Parameter Matrix and Results for Different Thermodynamic Properties. *Industrial and Engineering Chemistry Research*, *32*(1), 178–193. https://doi.org/10.1021/ie00013a024

Guichard, H., Lemesle, S., Ledauphin, J., Barillier, D., & Picoche, B. (2003). Chemical and Sensorial Aroma Characterization of Freshly Distilled Calvados. 1. Evaluation of Quality and Defects on the Basis of Key Odorants by Olfactometry and Sensory Analysis. *Journal of Agricultural and Food Chemistry*, *51*(2), 424–432. https://doi.org/10.1021/jf020372m

Guymon, J. F. (1974). Chemical Aspects of Distilling Wines into Brandy. In *Chemistry of Winemaking* (pp. 232–253). American Chemical Society. https://doi.org/10.1021/ba-1974-0137.ch011

Hodel, J., O'Donovan, T., & Hill, A. E. (2021). Influence of still design and modelling of the behaviour of volatile terpenes in an artificial model gin. *Food and Bioproducts Processing*, *129*(5), 46–64. https://doi.org/10.1016/j.fbp.2021.07.002

Ikari, A., & Kubo, R. (1975). Behavior of various impurities in simple distillation of aqueous solution of ethanol. *Journal of Chemical Engineering of Japan*, *8*(4), 294–299. https://doi.org/10.1252/jcej.8.294

International alcoholometric tables, OIML R22. (1975). International Organisation of Legal Metrology. https://www.oiml.org/en/files/pdf_r/r022-e75.pdf

Léauté, R. (1990). Distillation in alambic. *American Journal of Enology and Viticulture*, *41*(1), 90–103.

Luna, R., López, F., & Pérez-Correa, J. R. (2018). Minimizing methanol content in experimental charentais alembic distillations. *Journal of Industrial and Engineering Chemistry*, *57*, 160–170. https://doi.org/10.1016/j.jiec.2017.08.018

Luna, R., Matias-Guiu, P., López, F., & Pérez-Correa, J. R. (2019). Quality aroma improvement of Muscat wine spirits: A new approach using first-principles model-based design and multi-objective dynamic optimisation through multi-variable analysis techniques. *Food and Bioproducts Processing*, *115*, 208–222. https://doi.org/10.1016/j.fbp.2019.04.004

Lurton, L., Ferrari, G., & Snakkers, G. (2012). Cognac: Production and aromatic characteristics. In J. R. Piggott (Ed.), *Alcoholic Beverages: Sensory Evaluation and Consumer Research* (pp. 242–266). Woodhead Publishing Limited. http://dx.doi.org/10.1533/9780857095176.3.242

Ministère de l'agriculture et de la souveraineté alimentaire. (2022). Cahier des charges de l'appellation d'origine contrôlée «Cognac» ou «Eau-de-vie de Cognac» ou «Eau-de-vie des Charentes». In *BO AGRI*.

Muzenda, E. (2013). From UNIQUAC to Modified UNIFAC Dortmund : A Discussion. *3rd International Conference on Medical Sciences and Chemical Engineering (ICMSCE'2013)*, *5*, 32–41. http://psrcentre.org/images/extraimages/8 1213836.pdf

Osorio, D., Pérez-Correa, J. R., Biegler, L. T., & Agosin, E. (2005). Wine Distillates: Practical Operating Recipe Formulation for Stills. *Journal of Agricultural and Food Chemistry*, *53*(16), 6326–6331. https://doi.org/10.1021/jf047788f

Puentes, C., Joulia, X., Athès, V., & Esteban-Decloux, M. (2018a). Review and Thermodynamic Modeling with NRTL Model of Vapor-Liquid Equilibria (VLE) of Aroma Compounds Highly Diluted in Ethanol-Water Mixtures at 101.3 kPa. *Industrial and Engineering Chemistry Research*, *57*(10), 3443–3470. https://doi.org/10.1021/acs.iecr.7b03857

Puentes, C., Joulia, X., Vidal, J. P., & Esteban-Decloux, M. (2018b). Simulation of spirits distillation for a better understanding of volatile aroma compounds behavior: Application to Armagnac production. *Food and Bioproducts Processing*, *112*, 31–62. https://doi.org/10.1016/j.fbp.2018.08.010

Ramírez-Guízar, S., González-Alatorre, G., Pérez-Pérez, M. C. I., Piñeiro-García, A., & Lona-Ramírez, F. J. (2020). Identification and quantification of volatile toxic compounds in tequila. *Journal of Food Measurement and Characterization*, *14*(4), 2059–2066. https://doi.org/10.1007/s11694-020-00452-x

Sacher, J., García-Llobodanin, L., López, F., Segura, H., & Pérez-Correa, J. R. (2013). Dynamic modeling and simulation of an alembic pear wine distillation. *Food and Bioproducts Processing*, *91*(4), 447–456. https://doi.org/10.1016/j.fbp.2013.04.001

Scanavini, H. F. A., Ceriani, R., & Meirelles, A. J. A. (2012). Cachaça distillation investigated on the basis of model systems. *Brazilian Journal of Chemical Engineering*, *29*(2), 429–440. https://doi.org/10.1590/S0104-66322012000200022

Schaefer, J., & Timmer, R. (1970). Flavor Components in Cognac. *Journal of Food Science*, *35*(1), 10–12. https://doi.org/10.1111/j.1365-2621.1970.tb12356.x

Silva, M. L., & Malcata, F. X. (1999). Effects of time of grape pomace fermentation and distillation cuts on the chemical composition of grape marcs. *European Food Research and Technology*, *208*(2), 134–143. https://doi.org/10.1007/s002170050390

Spaho, N., Đukic-Ratković, D., Nikićević, N., Blesić, M., Tešević, V., Mijatović, B., & Smajić Murtić, M. (2019). Aroma compounds in barrel aged apple distillates from two different distillation techniques. *Journal of the Institute of Brewing*, *April 2018*, 389–397. https://doi.org/10.1002/jib.573

Thibaud, F., Courregelongue, M., & Darriet, P. (2020). Contribution of Volatile Odorous Terpenoid Compounds to Aged Cognac Spirits Aroma in a Context of Multicomponent Odor Mixtures. *Journal of Agricultural and Food Chemistry*, *68*(47), 13310–13318. https://doi.org/10.1021/acs.jafc.9b06656

Tsakiris, A., Kallithraka, S., & Kourkoutas, Y. (2014). Grape brandy production, composition and sensory evaluation. *Journal of the Science of Food and Agriculture*, *94*(3), 404–414. https://doi.org/10.1002/jsfa.6377

Tsakiris, A., Kallithraka, S., & Kourkoutas, Y. (2016). Brandy and Cognac: Manufacture and Chemical Composition. In *Encyclopedia of Food and Health* (3rd ed., Vol. 94, Issue 3, pp. 462–468). Elsevier. https://doi.org/10.1016/B978-0-12-384947-2.00081-7

Uselmann, V., & Schieberle, P. (2015). Decoding the combinatorial aroma code of a commercial cognac by application of the sensomics concept and first insights into

differences from a german brandy. *Journal of Agricultural and Food Chemistry*, *63*(7), 1948–1956. https://doi.org/10.1021/jf506307x

Valderrama, J. O., Faúndez, C. A., & Toselli, L. A. (2012). Advances on modeling and simulation of alcoholic distillation. Part 1: Thermodynamic modeling. *Food and Bioproducts Processing*, *90*(4), 819–831. https://doi.org/10.1016/j.fbp.2012.04.004

Waterhouse, A. L., Sacks, G. L., & Jeffery, D. W. (2016). Glycosidic Precursors to Wine Odorants. *Understanding Wine Chemistry*, 240–255. https://doi.org/10.1002/9781118730720.ch23a

Yuan, X., Zhou, J., Zhang, B., Shen, C., Yu, L., Gong, C., Xu, Y., & Tang, K. (2023). Identification, quantitation and organoleptic contributions of furan compounds in brandy. *Food Chemistry*, *412*(November 2022), 135543. https://doi.org/10.1016/j.foodchem.2023.135543

Zanghelini, G., Athès, V., Esteban-Decloux, M., Giampaoli, P., & Vitu, S. (2022a). Isobaric vapour-liquid equilibrium of α-terpineol highly diluted in hydroalcoholic mixtures at 101.3 kPa: Experimental measurements and thermodynamic modeling. *The Journal of Chemical Thermodynamics*, *171*, 106806. https://doi.org/10.1016/j.jct.2022.106806

Zanghelini, G., Esteban-Decloux, M., Vitu, S., Giampaoli, P., & Athès, V. (2022b). ß-Damascenone Highly Diluted in Hydroalcoholic Mixtures: Phase Equilibrium Measurements, Thermodynamic Modeling, and Simulation of a Batch Distillation. *Industrial & Engineering Chemistry Research*, *61*(49), 18127–18137. https://doi.org/10.1021/acs.iecr.2c01755

Zanghelini, G., Giampaoli, P., Athès, V., Vitu, S., Wilhelm, V. & Esteban-Decloux, M. (2024). *Charentaise distillation of cognac. Part I: behavior of aroma compounds* [Manuscript submitted for publication].

Zhao, Y., Tian, T., Li, J., Zhang, B., Yu, Y., Wang, Y., & Niu, H. (2014). Variations in main flavor compounds of freshly distilled brandy during the second distillation. *International Journal of Food Engineering*, *10*(4), 809–820. https://doi.org/10.1515/ijfe-2014-0123

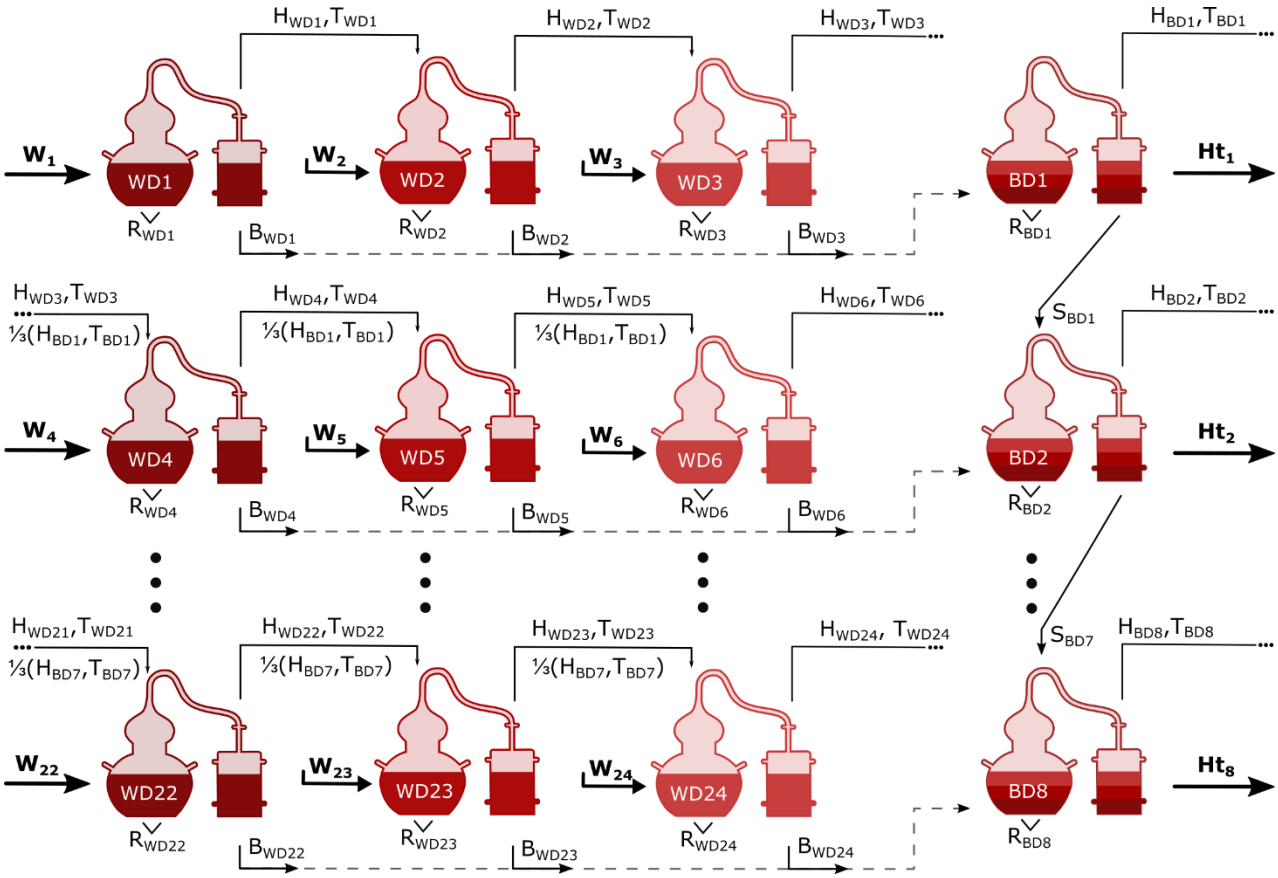

Figure 1. General scheme for modeling the recycling of distillate fractions for 24 WD and 8 BD.

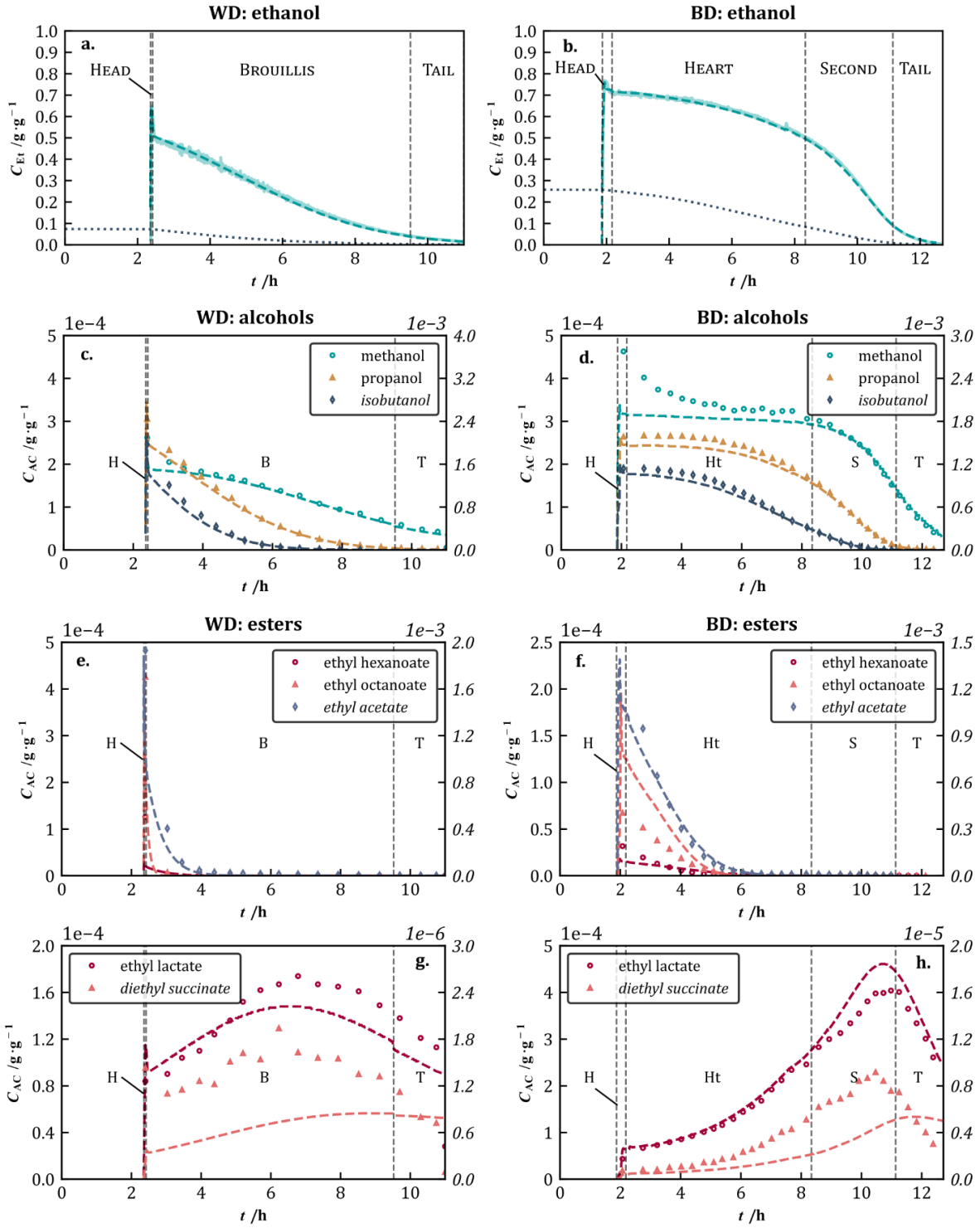

Figure 2. Concentration profiles of ethanol and various alcohols and esters during the WD (left hand side) and BD (right hand side). Distillate cuts are represented by vertical dashed lines: H, head; B, brouillis; T, tail; Ht, heart; S, second. Compounds projected in the secondary axis are italicized. In the two upper graphs (a,b), the continuous and the dashed lines (---) represent, respectively, the experimental and the simulated ethanol mass fractions in the distillate, whereas the dotted lines (···) are the ethanol concentrations in the boiler obtained from the simulation. In graphs (c-h), the hollow symbols represent the experimental concentrations of aroma compounds in the distillate, whereas the dashed lines (---) are the simulation data for the concentrations determined experimentally in the boiler load of the WD and the BD ($x_{0\,WD}$ and $x_{0\,BD}$).

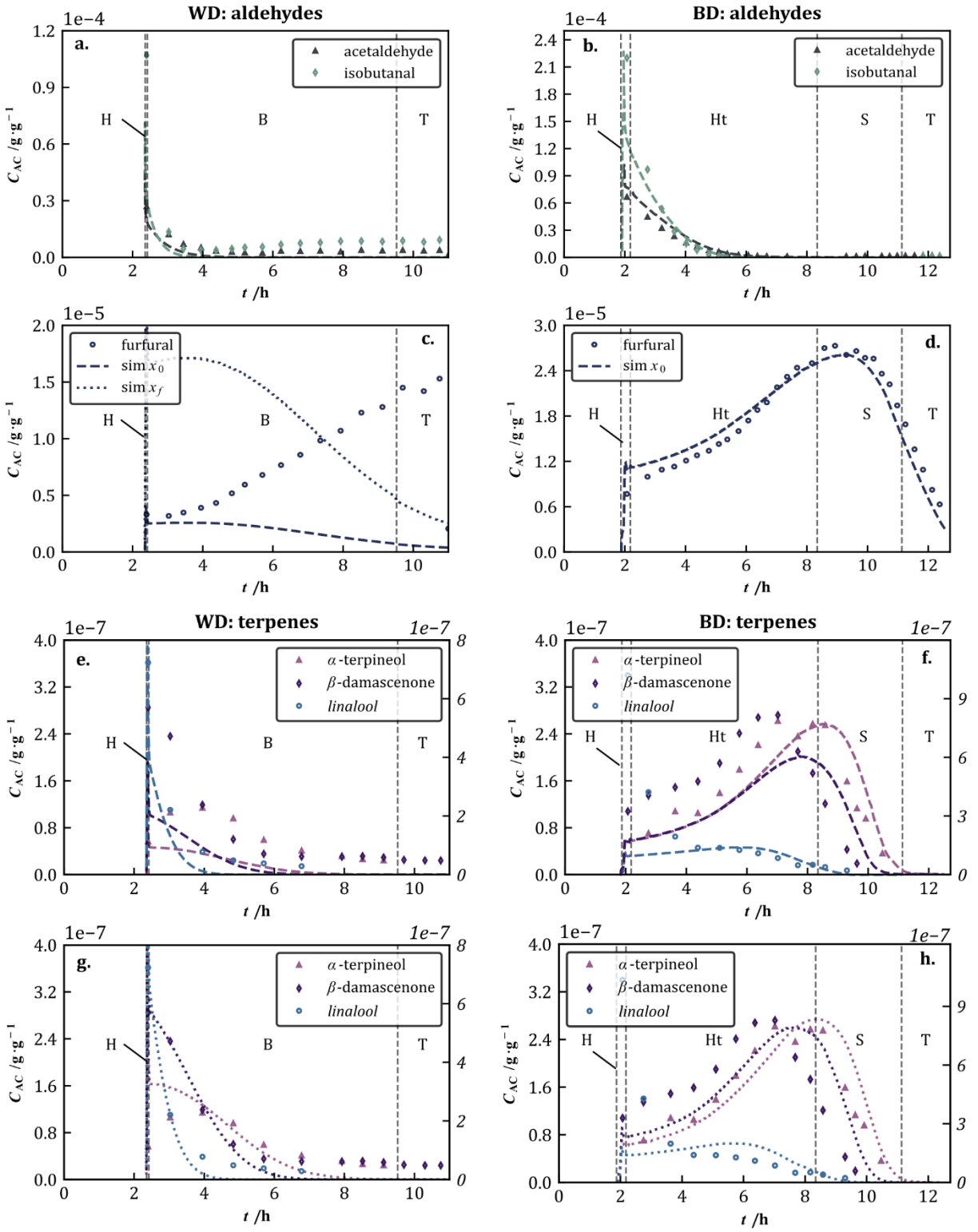

Figure 3. Concentration profiles in the WD and the BD for aroma compounds formed during distillation. Distillate cuts are represented by vertical dashed lines: H, head; B, brouillis; T, tail; Ht, heart; S, second. The hollow symbols represent the experimental concentrations of aroma compounds, whereas the dashed lines (---) and the dotted lines (···) represent, respectively, the simulation data using the initial concentrations in the boiler (x_0) and those calculated from the final masses (x_f).

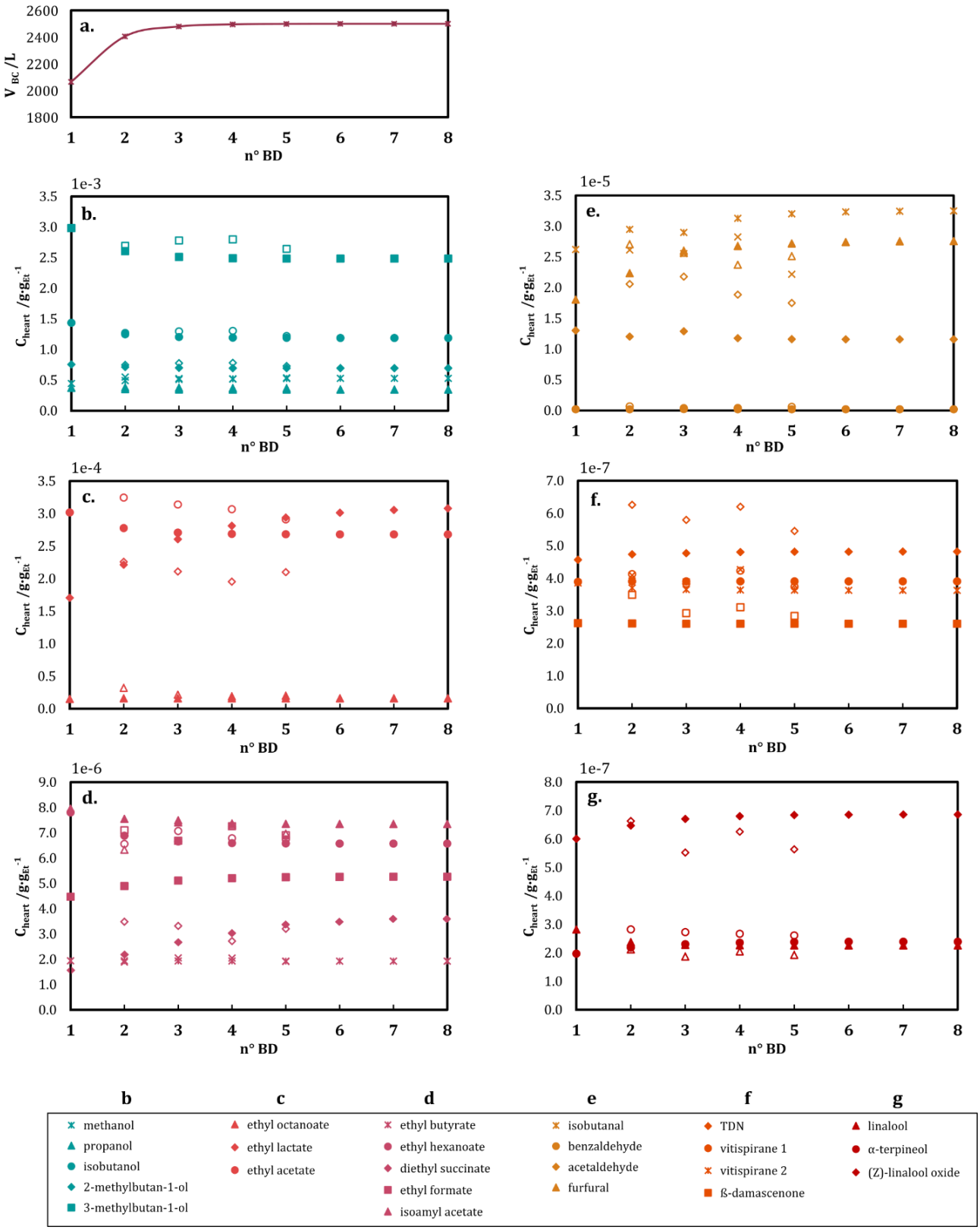

Figure 4. (a) Total volume loaded in the still for each BD and mass concentrations, in grams per gram of ethanol (g·g$_{Et}^{-1}$), of (b) alcohols, (c,d) esters, (e) aldehydes, (f) norisoprenoids and (g) terpenes in the heart of eight consecutive BD with recycling. Filled symbols correspond to the data estimated with the mathematical model, whereas hollow symbols are the experimental data from the heart samples collected on four consecutive days.

Table 1. Main simulation parameters for the wine and brouillis distillations.

	Wine distillation		Brouillis distillation	
Theoretical stages	7		7	
Liquid holdup				
· Condenser	1.0	L	1.0	L
· Trays 2 - 3	0.1	L	0.1	L
· Trays 4 - 6	0.5	L	0.2	L
Efficiency				
· Condenser	1.0		1.0	
· Trays 2 - 3	0.3		0.3	
· Trays 4 - 6	0.5		0.3	
· Boiler	1.0		1.0	
Pressure				
· Condenser	101.3	kPa	101.3	kPa
· Pressure loss	0		0	

Table 2. Composition of the loads for the simulations of the WD and the BD for the two calculation approaches: (1) based on the measured initial concentration (x_0) and (2) based on the concentrations, in **g·g^{-1},** estimated from the final masses of compounds (x_f).

		Load composition from m_0		Load composition from Σm_f	
Compounds	Model	$x_{0\,WD}$ (g·g^{-1})	$x_{0\,BD}$ (g·g^{-1})	$x_{f\,WD}$ (g·g^{-1})	$x_{f\,BD}$ (g·g^{-1})
Alcohols					
ethanol	NRTL	0.0738	0.2578	= $x_{0\,WD}$	= $x_{0\,BD}$
methanol	NRTL	4.35E-5	1.49E-4	= $x_{0\,WD}$	= $x_{0\,BD}$
propanol	NRTL	2.61E-5	8.29E-5	= $x_{0\,WD}$	= $x_{0\,BD}$
isobutanol	NRTL	9.02E-5	2.58E-4	= $x_{0\,WD}$	= $x_{0\,BD}$
butan-1-ol	NRTL	1.00E-8	1.00E-8	2.58E-7	6.44E-7
2-methylbutan-1-ol	NRTL	5.27E-5	1.50E-4	= $x_{0\,WD}$	= $x_{0\,BD}$
3-methylbutan-1-ol	NRTL	1.89E-4	5.52E-4	= $x_{0\,WD}$	= $x_{0\,BD}$
(*Z*)-3-hexenol	NRTL	2.72E-7	9.62E-7	= $x_{0\,WD}$	= $x_{0\,BD}$
hexanol	NRTL	1.14E-6	3.38E-6	= $x_{0\,WD}$	= $x_{0\,BD}$
2-phenylethanol	NRTL	2.61E-5	3.91E-5	= $x_{0\,WD}$	= $x_{0\,BD}$
octanol	UNIFAC	1.37E-8	3.85E-8	= $x_{0\,WD}$	= $x_{0\,BD}$
decanol	UNIFAC	6.72E-9	1.87E-8	= $x_{0\,WD}$	= $x_{0\,BD}$
dodecanol	UNIFAC	2.43E-9	1.56E-8	4.63E-9	= $x_{0\,BD}$
tetradecanol	UNIFAC	1.49E-8	2.10E-7	4.76E-8	= $x_{0\,BD}$
hexadecanol	UNIFAC	1.00E-8	9.89E-8	3.42E-8	1.53E-7
Esters					
ethyl formate	UNIFAC	1.00E-8	7.60E-7	4.00E-7	1.78E-6
ethyl acetate	NRTL	2.04E-5	6.76E-5	= $x_{0\,WD}$	= $x_{0\,BD}$
ethyl lactate	NRTL	5.45E-5	1.78E-4	= $x_{0\,WD}$	= $x_{0\,BD}$
isobutyl acetate	UNIFAC	1.00E-8	1.00E-8	2.49E-8	3.26E-7
ethyl butyrate	NRTL	1.47E-7	4.63E-7	= $x_{0\,WD}$	= $x_{0\,BD}$
isoamyl acetate	NRTL	5.59E-7	1.43E-6	3.84E-7	= $x_{0\,BD}$
ethyl 3-methylbutanoate	NRTL	6.79E-9	4.06E-8	4.44E-9	= $x_{0\,BD}$
diethyl succinate	NRTL	4.91E-7	2.63E-6	= $x_{0\,WD}$	= $x_{0\,BD}$
ethyl hexanoate	NRTL	5.00E-7	1.39E-6	3.32E-7	= $x_{0\,BD}$
hexyl acetate	NRTL	2.23E-8	4.89E-8	1.47E-8	= $x_{0\,BD}$
methyl salicylate	UNIFAC	1.75E-9	1.14E-8	3.94E-9	= $x_{0\,BD}$
2-phenylethyl acetate	NRTL	4.62E-8	2.28E-7	= $x_{0\,WD}$	= $x_{0\,BD}$
ethyl octanoate	NRTL	1.20E-6	6.97E-6	= $x_{0\,WD}$	4.25E-6
ethyl decanoate	NRTL	2.10E-6	1.89E-5	= $x_{0\,WD}$	9.87E-6
ethyl dodecanoate	UNIFAC	5.99E-7	6.27E-7	1.67E-6	9.07E-6
ethyl tetradecanoate	UNIFAC	6.93E-8	3.87E-6	6.03E-7	= $x_{0\,BD}$
ethyl linolenate	UNIFAC	8.26E-8	6.54E-7	3.47E-7	1.19E-6
ethyl linoleate	UNIFAC	3.11E-7	2.99E-6	1.37E-6	5.12E-6
ethyl oleate	UNIFAC	3.79E-8	4.07E-7	1.62E-7	6.97E-7
ethyl octadecanoate	UNIFAC	2.12E-8	4.02E-6	5.67E-8	2.98E-7
Aldehydes					
acetaldehyde	NRTL	4.80E-7	4.62E-6	2.30E-6	= $x_{0\,BD}$
isobutanal	NRTL	4.56E-7	5.59E-6	2.47E-6	= $x_{0\,BD}$

		Load composition from m_0		Load composition from Σm_f	
Compounds	Model	$x_{0\,WD}$ (g·g^{-1})	$x_{0\,BD}$ (g·g^{-1})	$x_{f\,WD}$ (g·g^{-1})	$x_{f\,BD}$ (g·g^{-1})
furfural	NRTL	6.05E-7	1.04E-5	4.00E-6	= $x_{0\,BD}$
benzaldehyde	UNIFAC	2.27E-8	8.33E-8	7.36E-8	1.46E-7
Terpenes and norisoprenoids					
(*E*)-ß-damascenone	NRTL	6.98E-9	5.21E-8	1.97E-8	= $x_{0\,BD}$
linalool	NRTL	1.00E-8	3.85E-8	1.71E-8	= $x_{0\,BD}$
α-terpineol	NRTL	5.17E-9	6.87E-8	1.82E-8	= $x_{0\,BD}$
(*Z*)-linalool oxide	NRTL	1.42E-8	8.12E-8	5.21E-8	1.62E-7
(*E*)-linalool oxide	NRTL	1.00E-9	5.93E-8	1.00E-9	= $x_{0\,BD}$
Acetals					
1,1-diethoxyethane	NRTL	2.85E-7	2.36E-6	9.24E-7	1.26E-6

Table 3. Representation of the experimental concentration profiles of aroma compounds by the computer simulation modules[a], taking into account for the boiler load the initial (x_0) or the final composition (x_f).

Compounds	Model	Fitting quality of concentration profiles			
		x_0 WD	x_0 BD	x_f WD	x_f BD
Alcohols					
ethanol	NRTL	+++	+++		
methanol	NRTL	++	+		
propanol	NRTL	+++	++		
isobutanol	NRTL	+++	++		
butan-1-ol	NRTL		>	+++	+
2-methylbutan-1-ol	NRTL	+++	+		
3-methylbutan-1-ol	NRTL	+++	+		
(*Z*)-3-hexenol	NRTL	+++	+		
hexanol	NRTL	Ø	Ø		
2-phenylethanol	NRTL	>	++		
octanol	UNIFAC	<	<		
decanol	UNIFAC	++	+		
dodecanol	UNIFAC	<	++	+++	
tetradecanol	UNIFAC	<	+	+	
hexadecanol	UNIFAC	<	>	+	+
Esters					
ethyl formate	UNIFAC	Ø	Ø	Ø	Ø
ethyl acetate	NRTL	+++	+++		
ethyl lactate	NRTL	<	++		
isobutyl acetate	UNIFAC		<	<	+
ethyl butyrate	NRTL	+++	+++		
isoamyl acetate	NRTL	<	++	<	
ethyl 3-methylbutanoate	NRTL	+	+	<	
diethyl succinate	NRTL	Ø	Ø		
ethyl hexanoate	NRTL	+	Ø	<	
hexyl acetate	NRTL	+	<	+	
methyl salicylate	UNIFAC	Ø	Ø	Ø	
2-phenylethyl acetate	NRTL	+	+		
ethyl octanoate	NRTL	++	>		++
ethyl decanoate	NRTL	++	>		+
ethyl dodecanoate	UNIFAC	>	<	>	>
ethyl tetradecanoate	UNIFAC	>	Ø	>	
ethyl linolenate	UNIFAC	Ø	Ø	>	Ø
ethyl linoleate	UNIFAC	Ø	Ø	>	Ø
ethyl oleate	UNIFAC	Ø	Ø	>	Ø
ethyl octadecanoate	UNIFAC	Ø	Ø	>	Ø

Compounds	Model	Fitting quality of concentration profiles			
		x_0 WD	x_0 BD	x_f WD	x_f BD
Aldehydes					
acetaldehyde	NRTL	<	+++	>	
isobutanal	NRTL	<	++	+	
furfural	NRTL	Ø	++	Ø	
benzaldehyde	UNIFAC	<	Ø	Ø	Ø
Terpenes and norisoprenoids					
(*E*)-ß-damascenone	NRTL	<	+	++	
linalool	NRTL	<	Ø	++	
α-terpineol	NRTL	<	++	+	
(*Z*)-linalool oxide	NRTL	<	Ø	<	Ø
(*E*)-linalool oxide	NRTL		++		
Acetals					
1,1-diethoxyethane	NRTL	<	>	+	+++

[a]Representation quality: great (+++), good (++), close (+), wrong shape (Ø), overestimated (>), underestimated (<).

Table 4. Distribution of aroma compounds between distillate fractions for the wine and brouillis distillations: experimental and simulation results.

		Wine distillation								Brouillis distillation									
	Thermodynamic model	Head (%)		Brouillis (%)		Tail (%)		Residue (%)		Head (%)		Heart (%)		Second (%)		Tail (%)		Residue (%)	
		Exp	Sim	Exp	Sim	Exp	Sim	Exp	Sim	Exp	Sim	Exp	Sim	Exp	Sim	Exp	Sim	Exp	Sim
Alcohols																			
ethanol	NRTL	1.4	1.4	95.9	95.9	1.7	1.7	1.0	1.0	2.1	2.1	75.1	75.2	21.2	21.1	1.6	1.4	0.0	0.1
methanol	NRTL	1.1	0.8	85.9	88.6	4.9	6.3	8.1	4.4	2.2	1.6	65.2	62.4	26.9	28.8	5.7	5.6	0.0	1.6
propanol	NRTL	2.1	1.9	96.5	97.7	0.6	0.3	0.8	0.1	2.2	2.2	81.8	81.3	14.7	16.2	0.5	0.4	0.8	0.0
isobutanol	NRTL	4.1	3.3	95.5	96.7	0.0	0.0	0.4	0.0	3.1	3.0	92.0	91.0	4.9	5.9	0.0	0.0	0.0	0.0
butan-1-ol	NRTL	-	2.5	-	97.3	-	0.0	-	0.2	2.1	2.1	97.9	85.8	0.0	12.0	0.0	0.1	0.0	0.0
2-methylbutan-1-ol	NRTL	4.7	3.8	94.9	96.2	0.0	0.0	0.4	0.0	2.5	2.5	93.1	93.1	4.4	4.4	0.0	0.0	0.0	0.0
3-methylbutan-1-ol	NRTL	4.0	3.4	95.6	96.6	0.0	0.0	0.4	0.0	2.1	2.5	91.2	90.7	6.6	6.9	0.0	0.0	0.2	0.0
(*Z*)-3-hexenol	NRTL	2.2	2.3	97.8	97.7	0.0	0.0	0.0	0.0	1.0	1.3	70.4	80.6	28.3	18.0	0.3	0.1	0.0	0.0
hexanol	NRTL	4.3	1.5	95.7	97.8	0.0	0.7	0.0	0.0	1.4	1.2	90.5	71.3	6.7	26.5	1.4	0.9	0.0	0.0
2-phenylethanol	NRTL	0.2	0.0	39.6	50.7	9.2	14.8	51.0	34.5	0.1	0.0	8.5	7.5	25.4	34.8	25.5	26.0	40.6	31.6
octanol	UNIFAC	9.0	3.4	91.0	96.6	0.0	0.0	0.0	0.0	2.7	1.4	92.4	86.3	4.9	12.3	0.0	0.0	0.0	0.1
decanol	UNIFAC	13.8	4.9	86.2	95.1	0.0	0.0	0.0	0.0	3.2	1.3	92.7	91.1	2.9	7.4	1.3	0.0	0.0	0.2
dodecanol	UNIFAC	7.2	7.0	92.8	92.9	0.0	0.0	0.0	0.0	5.4	1.2	91.7	94.7	0.0	4.0	2.9	0.0	0.0	0.1
tetradecanol	UNIFAC	4.7	11.8	79.4	88.2	2.4	0.0	13.4	0.0	1.3	1.4	85.2	97.6	9.5	0.8	1.3	0.0	2.7	0.2
hexadecanol	UNIFAC	5.8	17.8	91.4	82.2	2.8	0.0	0.0	0.0	3.1	1.4	78.7	98.4	6.8	0.1	1.1	0.0	10.4	0.0
Esters																			
ethyl formate	UNIFAC	4.7	5.4	95.3	94.5	0.0	0.0	0.0	0.0	19.3	8.1	64.3	91.6	16.4	0.3	0.0	0.0	0.0	0.0
ethyl acetate	NRTL	18.3	9.8	80.0	90.0	0.6	0.0	1.0	0.1	18.1	12.9	80.2	86.6	1.4	0.0	0.3	0.0	0.0	0.4
ethyl lactate	NRTL	0.2	0.2	60.6	67.9	8.9	12.7	30.3	19.2	0.2	0.2	24.6	23.9	37.4	41.7	22.7	19.6	15.0	14.7
isobutyl acetate	UNIFAC	-	24.1	-	75.7	-	0.0	-	0.1	13.8	18.2	86.2	81.8	0.0	0.0	0.0	0.0	0.0	0.0
ethyl butyrate	NRTL	54.5	22.2	45.5	77.6	0.0	0.0	0.0	0.2	22.9	17.3	75.9	82.5	1.2	0.0	0.0	0.0	0.0	0.2
isoamyl acetate	NRTL	64.7	16.7	35.3	83.1	0.0	0.0	0.0	0.2	20.8	13.7	79.2	86.3	0.0	0.0	0.0	0.0	0.0	0.0
ethyl 3-methylbutanoate	NRTL	-	19.9	-	80.1	-	0.0	-	0.0	17.8	13.3	74.7	86.7	7.5	0.0	0.0	0.0	0.0	0.0
diethyl succinate	NRTL	0.5	0.1	78.1	38.4	7.9	12.3	13.5	49.3	0.2	0.1	21.6	11.9	54.0	27.1	18.2	19.9	6.1	40.9
ethyl hexanoate	NRTL	68.8	8.4	30.4	91.4	0.0	0.0	0.8	0.2	17.7	8.7	78.7	91.3	3.3	0.1	0.3	0.0	0.0	0.0
hexyl acetate	NRTL	67.0	15.9	33.0	84.2	0.0	0.0	0.0	0.0	15.4	7.7	84.6	92.3	0.0	0.0	0.0	0.0	0.0	0.0
methyl salicylate	UNIFAC	0.0	0.1	87.3	60.8	12.7	10.1	0.0	29.0	0.0	0.1	85.0	15.8	15.0	41.9	0.0	22.9	0.0	19.3
2-phenylethyl acetate	NRTL	0.0	2.3	0.0	97.7	0.0	0.0	0.0	0.0	1.0	0.4	62.6	66.4	35.6	33.2	0.9	0.0	0.0	0.0
ethyl octanoate	NRTL	0.0	38.4	97.1	61.5	0.5	0.0	2.4	0.1	12.6	13.2	82.5	86.8	4.6	0.0	0.2	0.0	0.0	0.0

		Wine distillation								Brouillis distillation									
	Thermodynamic model	Head (%)		Brouillis (%)		Tail (%)		Residue (%)		Head (%)		Heart (%)		Second (%)		Tail (%)		Residue (%)	
		Exp	Sim	Exp	Sim	Exp	Sim	Exp	Sim	Exp	Sim	Exp	Sim	Exp	Sim	Exp	Sim	Exp	Sim
ethyl decanoate	NRTL	53.1	44.5	34.8	55.5	5.6	0.0	6.6	0.0	7.4	9.4	69.4	90.6	2.7	0.0	1.5	0.0	19.0	0.0
ethyl dodecanoate	UNIFAC	31.3	68.5	61.0	31.5	0.1	0.0	7.6	0.0	7.1	0.6	91.8	3.5	0.6	0.0	0.0	0.0	0.5	95.9
ethyl tetradecanoate	UNIFAC	6.2	88.9	88.4	11.4	1.0	0.0	4.5	0.0	5.5	18.9	92.9	81.1	0.8	0.0	0.1	0.0	0.8	0.0
ethyl linolenate	UNIFAC	7.6	100.0	86.1	0.0	2.6	0.0	3.8	0.0	5.1	21.0	81.1	79.0	10.2	0.0	0.6	0.0	2.9	0.0
ethyl linoleate	UNIFAC	6.9	100.0	84.9	0.0	3.6	0.0	4.7	0.0	6.4	27.3	83.4	72.7	4.9	0.0	0.7	0.0	4.7	0.0
ethyl oleate	UNIFAC	6.3	100.0	84.7	0.0	4.3	0.0	4.7	0.0	7.3	47.6	82.6	52.4	2.6	0.0	0.5	0.0	6.9	0.0
ethyl octadecanoate	UNIFAC	7.7	100.0	79.3	0.0	5.0	0.0	7.9	0.0	7.4	30.7	79.9	69.3	0.9	0.0	0.6	0.0	11.2	0.0
Aldehydes																			
acetaldehyde	NRTL	2.1	8.3	54.2	91.7	7.4	0.0	36.3	0.0	9.3	13.6	55.4	86.4	4.8	0.0	4.6	0.0	25.9	0.0
isobutanol	NRTL	7.8	14.0	74.9	85.9	17.3	0.0	0.0	0.0	31.2	18.4	67.3	81.6	0.0	0.0	1.5	0.0	0.0	0.0
furfural	NRTL	0.1	0.8	48.4	91.7	16.5	5.0	34.9	2.5	0.5	0.7	47.0	51.2	40.9	40.0	11.6	6.8	0.0	1.3
benzaldehyde	UNIFAC	2.8	4.4	28.8	95.6	0.0	0.0	68.5	0.0	1.9	3.1	49.2	93.2	21.1	3.7	3.6	0.0	24.2	0.0
Terpenes and norisoprenoids																			
(*E*)-ß-damascenone	NRTL	2.6	2.9	91.6	97.1	5.8	0.0	0.0	0.0	1.2	0.8	91.2	75.8	7.6	23.4	0.0	0.0	0.0	0.0
linalool	NRTL	7.6	8.5	92.4	91.6	0.0	0.0	0.0	0.0	14.9	1.8	80.4	96.2	4.1	2.0	0.6	0.0	0.0	0.0
α-terpineol	NRTL	0.6	1.7	99.4	98.3	0.0	0.0	0.0	0.0	2.9	0.5	68.3	61.7	27.5	37.6	1.3	0.2	0.0	0.0
(*Z*)-linalool oxide	NRTL	25.4	2.1	69.2	97.7	5.4	0.0	0.0	0.2	26.7	0.6	53.4	65.7	18.5	33.7	1.5	0.0	0.0	0.0
(*E*)-linalool oxide	NRTL	-	2.1	-	97.7	-	0.0	-	0.2	1.0	0.6	51.2	65.7	44.9	33.7	2.8	0.0	0.0	0.0
Acetals																			
1,1-diethoxyethane	NRTL	3.5	6.4	43.1	93.4	0.0	0.0	53.3	0.2	19.6	12.1	73.1	87.8	0.0	0.1	7.3	0.0	0.0	0.0

Table 5. Effect of different recycling configurations after 8 successive Charentaise distillations in the extraction percentage of each compound in the heart of BD n°8 in relation to their initial mass in the wine.

Alcohols	Rep[1]	R-HST (%)	NR (%)	R-HST$_{WD}$ (%)	R-ST (%)	R-S (%)
ethanol	sim	98.8	72.1	98.5	94.8	91.5
methanol	sim	92.4	55.2	90.5	89.4	77.6
propanol	sim	99.9	79.4	99.9	95.5	94.8
isobutanol	sim	100.0	88.0	100.0	93.5	93.5
butan-1-ol	sim	99.8	83.5	99.8	94.9	94.9
2-methylbutan-1-ol	sim	100.0	78.7	100.0	94.1	93.9
3-methylbutan-1-ol	sim	100.0	87.6	100.0	94.0	94.0
(*Z*)-3-hexenol	sim	100.0	78.7	100.0	96.1	96.0
hexanol	exp	100.0	86.6	100.0	94.2	92.8
2-phenylethanol	sim	9.0	3.8	7.0	9.0	5.9
octanol	sim	99.9	83.3	99.9	95.0	95.0
decanol	sim	99.7	86.6	99.7	93.5	93.5
dodecanol	sim	99.9	88.0	99.9	91.7	91.7
tetradecanol	sim	99.8	86.1	99.8	86.8	86.8
farnesol	exp	65.4	44.9	58.4	62.1	60.5
hexadecanol	exp	88.3	71.9	88.3	80.2	77.1
Esters	Rep[1]	R-HST (%)	NR (%)	R-HST$_{WD}$ (%)	R-ST (%)	R-S (%)
ethyl formate	exp	100.0	61.3	100.0	73.4	73.4
ethyl acetate	sim	99.9	78.4	99.9	78.4	78.4
ethyl lactate	sim	42.9	16.2	35.6	42.6	27.8
ethyl butyrate	exp	99.7	64.1	99.7	64.1	64.1
isoamyl acetate	sim	99.7	71.7	99.7	71.7	71.7
ethyl 3-methylbutanoate	sim	100.0	69.5	100.0	69.5	69.5
ethyl furoate	exp	100.0	61.1	100.0	96.7	94.8
diethyl succinate	exp	57.4	16.9	47.1	56.7	36.4
ethyl hexanoate	sim	99.7	83.4	99.7	83.5	83.5
hexyl acetate	sim	100.0	77.6	100.0	77.6	77.6
methyl salicilate	exp	100.0	74.2	100.0	100.0	87.3
2-phenylethyl acetate	sim	99.8	64.7	99.7	96.9	96.8
2-phenylethyl octanoate	sim	100.0	69.5	100.0	94.9	91.6
ethyl octanoate	sim	99.9	53.3	99.9	53.3	53.3
isobutyl decanoate	exp	88.0	46.1	87.8	47.2	47.1
ethyl decanoate	sim	100.0	50.3	100.0	50.3	50.3
ethyl dodecanoate	exp	87.7	56.0	87.7	56.4	56.3
isoamyl decanoate	sim	92.8	65.9	92.8	66.0	66.0
ethyl tetradecanoate	exp	94.1	82.1	94.1	83.6	82.8
farnesyl acetate	exp	80.4	68.1	79.0	74.2	74.2
isoamyl dodecanoate	exp	95.6	82.1	95.6	84.0	82.3
ethyl hexadecanoate	exp	91.0	78.0	90.9	82.1	78.8
ethyl linolenate	exp	92.2	69.8	91.7	80.3	77.8
ethyl linoleate	exp	89.4	70.8	89.1	77.7	74.4

ethyl oleate	exp	87.0	70.0	86.9	75.5	71.9
ethyl octadecanoate	exp	79.1	63.4	79.0	67.6	63.9
Aldehydes	Rep[1]	R-HST (%)	NR (%)	R-HST$_{WD}$ (%)	R-ST (%)	R-S (%)
acetaldehyde	exp	38.2	30.0	37.4	35.1	31.5
isobutanal	exp	99.9	50.4	100.0	61.8	50.4
furfural	exp	52.3	22.8	39.4	51.9	38.4
benzaldehyde	exp	18.8	14.1	15.8	18.2	17.9
Norisoprenoids	Rep[1]	R-HST (%)	NR (%)	R-HST$_{WD}$ (%)	R-ST (%)	R-S (%)
TDN	exp	95.6	58.5	95.4	63.7	60.8
(*E*)-ß-damascenone	sim	100.0	73.8	100.0	96.2	96.2
vitispirane 1	exp	100.0	70.7	100.0	80.6	79.2
vitispirane 2	exp	100.0	74.2	100.0	76.4	76.1
Terpenes	Rep[1]	R-HST (%)	NR (%)	R-HST$_{WD}$ (%)	R-ST (%)	R-S (%)
linalool	sim	100.0	88.1	100.0	89.9	89.9
α-terpineol	sim	99.9	60.6	99.9	97.5	97.2
(*Z*)-linalool oxide	sim	99.8	64.2	99.7	97.0	96.9
(*E*)-linalool oxide	sim	100.0	64.4	100.0	97.2	97.1
(*E*)-nerolidol	exp	70.2	58.8	68.6	63.3	63.3
Acetals	Rep[1]	R-HST (%)	NR (%)	R-HST$_{WD}$ (%)	R-ST (%)	R-S (%)
1,1-diethoxyethane	exp	37.2	31.5	37.2	32.6	31.5
1,1-diethoxyisobutane	exp	89.3	43.4	89.2	48.5	44.2

[1]The repartition adopted for each compound: exp, experimental; sim, simulation. R-HST, recycling of heads + tails in the WD and second in the BD; NR, no recycling; R-HST$_{WD}$, recycling of heads + tails + second in the WD; R-ST, recycling of tails in the WD and second in the BD; R-S, recycling of second in the BD.